Available online at www.sciencedirect.com

ScienceDirect

Scripta Materialia 70 (2014) 39–42

Scripta MATERIALIA

www.elsevier.com/locate/scriptamat

High strength and ductility of friction-stir-welded steel joints due to mechanically stabilized metastable austenite

Hidetoshi Fujii,[a,*] Rintaro Ueji,[a] Yoshiaki Morisada[a] and Hiroyasu Tanigawa[b]

[a]*Joining and Welding Research Institute, Osaka University, 11-1, Mihogaoka, Ibaraki, Osaka 567-0047, Japan*
[b]*Japan Atomic Energy Agency, 2-166, Obuchi-Omotedate, Rokkasho, Aomori 039-3212, Japan*

Received 31 August 2013; revised 9 September 2013; accepted 10 September 2013
Available online 18 September 2013

Steel plates were friction-stir-welded together under conditions in which samples were first heated above the lower critical temperature of the alloy and subsequently cooled at approximately 100 K s^{-1}. This method produced joints with an excellent balance between tensile strength and ductility. Severe plastic deformation during friction-stir-welding stabilized the austenite phase in the steel joints. The austenite phase was subsequently transformed through deformation into the martensite phase when the joints were actually used.

Keywords: Friction stir welding; Steels; Mechanical properties; Microstructure; Phase transformation

Welding and joining are multibillion-dollar fabrication technologies extensively used in the construction, transport, aerospace, energy, shipbuilding and electronics industries [1]. However, the material properties of steel generally deteriorate as steel parts are welded and joined together. Accordingly, there have previously been numerous attempts to minimize the deterioration of the mechanical properties of steel joints. We demonstrate for the first time ever that friction-stir-welding (FSW) can produce a mechanically stabilized metastable austenite phase that actually increases the elongation and tensile strength of steel joints.

FSW is a revolutionary method of solid-state joining that was invented in the UK [2]. In FSW, a 10–20 mm diameter rod-like tool rotating at high speed is pressed onto the surface of the material to be joined where it generates frictional heat. The tool is then moved along the interface of the material to join parts together. Because the maximum temperature of FSW is below the melting point of the material, joints produced using FSW exhibit material properties that are superior to those of the base metal. Therefore, FSW has recently been used for a wide variety of low-melting-point materials such as Al, Mg and Cu alloys [3–12]. Application of FSW to various steels has become possible through the development of appropriate tools and because of work that has been done to determine the appropriate welding conditions [13–22].

Several of the authors have previously used FSW to develop a method of welding together plain carbon steel parts below the lower critical temperature, A_{C1} (726 °C), of carbon steel [19–21]. A joint without a martensite structure is produced even when the method is used to weld together parts produced with hypereutectoid steel (0.85 wt.% C, AISI-1080). Such steel is very difficult to weld using conventional methods of welding because phase transformation causes cracks to form in the steel. However, the authors believed that a method of welding such as FSW, which does not induce phase transformation, could be used to weld such steel while retaining the toughness of welded high-carbon steel joints. Joints produced using the method they developed exhibited mechanical properties that are superior to those of joints produced using conventional methods of welding. When the method was extended to welding other difficult-to-weld metals, we found that although the austenite phase in steel is completely unstable at room temperature, FSW significantly stabilizes the austenite phase against the martensite reaction at room temperature, which is an interesting and completely unexpected phenomenon.

The chemical composition of the steel alloy used in this study was 0.1 C, 8 Cr, 2 W, 0.2 V, 0.04 Ta (wt.%), and the balance was Fe. This steel consists of

* Corresponding author. Tel./fax: +81 6 6879 8643; e-mail: fujii@jwri.osaka-u.ac.jp

1359-6462/$ - see front matter
http://dx.doi.org/10.1016/j.scriptamat.2013.09.012

ferrite and tempered martensite phases and can be categorized as high-chromium ferritic steel. The A_{C1} temperature of this alloy is 850 °C based on dilatometry. High-chromium steel is difficult to weld because of the precipitation of brittle phases, which is why the authors selected this particular steel for this study. FSW was conducted under the following conditions: the rotating tool was made of cemented carbide (i.e. tungsten carbide, WC), which has high strength, high toughness and good thermal conductivity in the range of welding temperatures anticipated in this study. The tool had a 12 mm diameter shoulder and a probe 4 mm in diameter and 1.4 mm long was used at a tilt of 3° from the normal to the plate. FSW was performed at rotational speeds of 100–300 rpm and at a constant welding speed of 100 mm min^{-1}. Argon was used as a shielding gas at a flow rate of 30 l min^{-1} to prevent oxidation of the steel and the tool during FSW.

Frigaard et al. [23] reported that the total amount of heat generated during FSW, q_0, can be given by the following equation:

$$q_0 = \int_0^R 4\pi^2 \mu P N r^2 dr = \frac{4}{3}\pi^2 \mu P N R^3, \quad (1)$$

where μ is the friction coefficient, R (m) is the surface radius, N (s^{-1}) is the rotation speed and P (N m^{-3}) is the mean pressure at the interface between the tool and joint. Eq. (1) can be used to control heat generation by varying N while fixing μ, P and R, i.e. more heat is input into a joint with increasing N.

The mechanical properties of the joints welded together at each N were assessed by tensile testing at a quasi-static strain rate. In addition, the macrostructures of cross-sections of the joint cut perpendicular to the FSW direction were observed by optical microscopy and scanning electron microscopy (SEM) using a microscope equipped with an electron backscatter diffraction (EBSD) detector. Each cross-section was polished to a mirror finish and was then etched using Keller's solution (95% HNO_3 + 1% C_2H_5OH + 1.5% HF + 2.5% HCl).

Figure 1 shows the microstructures of cross-sections of the joints welded together at each N. Defect-free joints were obtained at each N. The welding temperature was above the A_{C1} transformation point when $N = 300$ rpm and the stir zone whitened, indicating the formation of a phase distinguishable from the one that had formed below A_{C1} and that was indicated by a peripheral dark area. When $N = 200$ rpm, the welding was performed above A_{C1} from the top to the middle of the stir zone and below A_{C1} from the middle to the bottom of the stir zone. Accordingly, the boundary between the white and dark areas is observed in the central part of the stir zone. When $N = 100$ rpm, on the other hand, the entire stir zone was formed below A_{C1}, and no such boundary was observed.

The maximum welding temperatures were measured at the centre back surfaces of the butt samples. The temperatures were 740, 762, and 787 °C when $N = 100$, 200, and 300 rpm, respectively. The maximum welding temperature was below the A_{C1} temperature when $N = 100$ and 200 rpm, and above it when $N = 300$ rpm. The cooling rate decreased with increasing rotation speed. When the cooling rate is defined as the average cooling rate from the maximum temperature to 500 °C, the cooling rate was 58, 78 and 120 °C s^{-1} when $N = 100$, 200 and 300 rpm, respectively. FSW was performed in the single-γ phase or (α + γ) phase temperature regions when $N = 300$ rpm. When $N = 100$ rpm, on the other hand, it was performed without any phase transformation. However, the temperature was measured at the bottom of the plates; therefore, it is necessary to examine the microstructure to determine whether the phase actually transforms during FSW.

Figure 2 shows the phase maps obtained for the central part of the stir zone by measuring the EBSD of the joints when $N = 100$–300 rpm. There is a microstructure boundary at the centre of the stir zone when $N = 200$ rpm, as previously mentioned. Accordingly, the phase maps for both the upper and lower parts of the stir zone are shown. Body-centred cubic (bcc) ferrite

Rotation speed (rpm)	Welding speed (mm/min)	RS Cross-Section AS
100	100	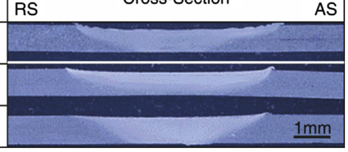
200	100	
300	100	1mm

Figure 1. Cross-sections of joints welded at various rotation speeds and at a constant welding speed of 100 mm min^{-1}. At a rotation speed of 100 rpm, the entire stir zone was dark white and was formed at temperature below A_{C1}. At rotation speed of 300 rpm, however, the stir zone was white when formed at a temperature above A_{C1}. At a rotation speed of 200 rpm, the welding temperature was above A_{C1} in the upper part of stir zone and below A_{C1} in the lower part.

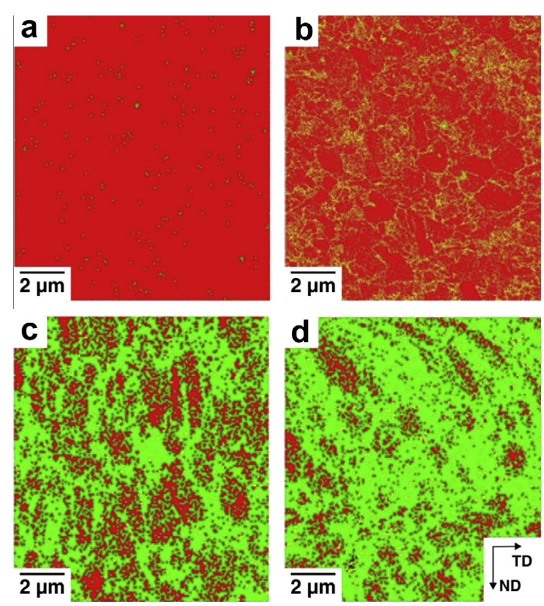

Figure 2. Phase maps for joints friction-stir-welded at rotation speeds of (a) 100, (b) 200 (lower stir zone), (c) 200 (upper stir zone) and (d) 300 rpm. Red and green indicate ferrite and austenite phases, respectively, and yellow points denote locations where phase cannot be precisely determined. (For interpretation of the references to colour in this figure legend, the reader is referred to the web version of this article.)